

Journal notes on:

Introduction to topological superconductivity

by Francisco Lobo



CONTENTS

I.	Introduction to superconductivity theory	3
A.	London theory	3
B.	BCS theory	3
C.	Ginzburg-Landau theory	3
1.	Classic type II superconductors	3
2.	Josephson effect	3
D.	Time-dependent Ginzburg-Landau theory	3
II.	Introduction to topological superconductivity	3
A.	Concepts of topology and symmetry	3
1.	Topological invariant	3
2.	Unitary symmetry (US)	4
3.	Time-reversal symmetry	4
4.	Sublattice symmetry	5
5.	Particle-hole symmetry	5
B.	One-dimensional system	7
1.	Ising model	7
2.	Hubbard model	7
3.	Kitaev model	7
4.	SSH model	11
5.	Oreg-Lutchyn model	11
C.	Hall effects	15
1.	Integer quantum Hall effect	15
2.	Quantum spin Hall (Kane-Mele) effect	15
3.	Quantum anomalous Hall effect	15
4.	Fraction Hall effect	15
D.	Graphene	15
1.	Monolayer graphene	15
2.	Bilayer Bernal graphene	18
3.	Haldane model	20
4.	Kekulé modulation	20
5.	Twisted bilayer graphene	20

I. INTRODUCTION TO SUPERCONDUCTIVITY THEORY

This chapter closely follows "Introduction to superconductivity" by Tinkham - Dover Publications 9780486435039.

A. London theory

B. BCS theory

C. Ginzburg-Landau theory

1. Classic type II superconductors

2. Josephson effect

D. Time-dependent Ginzburg-Landau theory

II. INTRODUCTION TO TOPOLOGICAL SUPERCONDUCTIVITY

Not a linear story telling of topological superconductivity theory per say, more of a compilation of different models that spark interest due to their topological and superconductive properties. Each section are mostly self contained, having their own bibliography at the start. This chapter closely follows Akhmerov's "Online course on topology in condensed matter" at <https://topocondmat.org/>.

As supplementary material, there is a GitHub repository at <https://github.com/franciscolobo1880/topoSC> where you can check the code that generate the figures of the various models. This is done in *Julia* using the *Quantica.jl* package by Pablo San-Jose, my PhD advisor. Check *Quantica.jl*'s repository and it's tutorial at <https://github.com/pablosanjose/Quantica.jl>.

A. Concepts of topology and symmetry

1. Topological invariant

Topology studies whether objects can be transformed continuously into each other. In condensed matter physics we can ask whether the Hamiltonians of two different systems can be continuously transformed into each other. If that is the case, then we can say that two systems are ‘topologically equivalent’.

In order to understand the concept of topology in condensed matter in the simplest way possible let us consider the deformation of a system described by the Hamiltonian H by the tuning of some external parameter α such that at $H_i \equiv H(\alpha = 0)$ is the initial state Hamiltonian and $H_f \equiv H(\alpha = 1)$ the final. If we consider absolutely no constraint then every H_i could be continuously deformed into H_f , meaning that they are always topologically equivalent. However, if H is, for example, forced to maintain a (physically) finite energy gap or is constrained by some symmetry considerations, then telling if they are topologically equivalent is not trivial. For this, let us imagine a panoply of different example of energy spectrums as a function of α and let us count the number of levels below zero energy at each different α , denoting it with Q . This will be our topological invariant prototype. If Q is the same in the initial and final system and did not change along the tuning of α then there must be a continuous transformation Hamiltonian which does not close the gap. One the other hand, if Q changes

then the system are *not* topologically equivalent as it would be needed to close the (physically real) gap. Hence, such a crossing changes the topological invariant, dubbed topological phase transition.

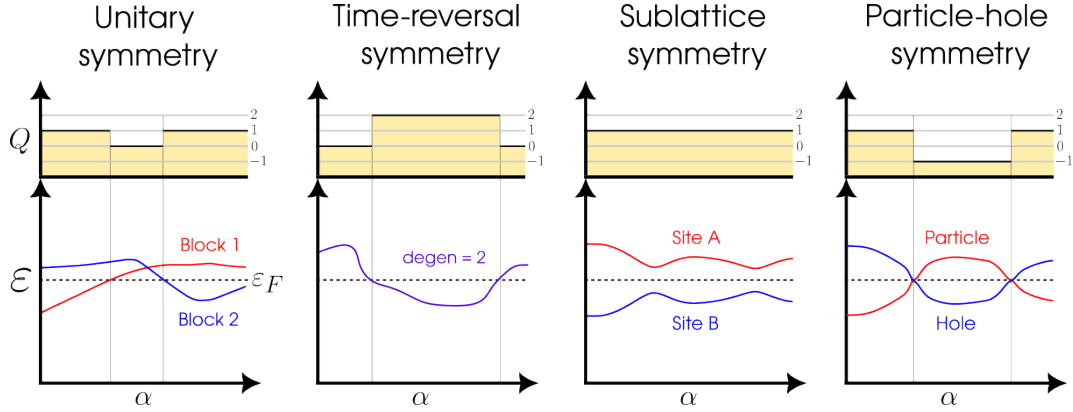


Figure 1. Kitaev chain Majorana modes pairing possibilities

2. Unitary symmetry (US)

Consider now that the Hamiltonian \mathcal{H} has the symmetry constraint $U^\dagger \mathcal{H} U = \mathcal{H}$ with U an unitary transformation. Hence \mathcal{H} commutes with U thus sharing common eigenenergies. This means that the system has a conservation law, and that the Hamiltonian can be brought to a block-diagonal form

$$\mathcal{H} = \left(\begin{array}{c|c} \mathcal{H}_A & \\ \hline & \mathcal{H}_B \end{array} \right) = \left(\begin{array}{cc|cc} a_{11} & a_{12} & 0 & 0 \\ a_{12}^* & a_{22} & 0 & 0 \\ \hline 0 & 0 & b_{11} & b_{12} \\ 0 & 0 & b_{12}^* & b_{22} \end{array} \right). \quad (1)$$

The band spectrum versus α and the topological invariant Q of each block can then be looked at individually and combined to get the full picture, as shown in Fig.(1).

Unitary symmetries play a rather boring role. They allow to reduce the dimension of the problem at hand, but nothing more. There are however other symmetries which can have a rich influence on topology.

3. Time-reversal symmetry

Time-reversal symmetry is represented by an anti-unitary operator, and as such it can always be written as the product $\mathcal{T} = UK$ with U an unitary matrix and K complex conjugation. For example, for a spinless system we have $\mathcal{T} = K$ and thus $\mathcal{T}\mathcal{H}\mathcal{T}^{-1} = \mathcal{H}^* = \mathcal{H}$. A real Hamiltonian is a manifestation of time-reversal symmetry. Such a Hamiltonian would read in matrix form as

$$\mathcal{H} = \left(\begin{array}{c|c} \mathcal{H}_A & M \\ \hline M^\dagger & \mathcal{H}_B \end{array} \right) = \left(\begin{array}{cc|cc} a_{11} & a_{12} & m_{11} & m_{12} \\ a_{12}^* & a_{22} & m_{21} & m_{22} \\ \hline m_{11}^* & m_{21}^* & b_{11} & b_{12} \\ m_{12}^* & m_{22}^* & b_{12}^* & b_{22} \end{array} \right). \quad (2)$$

where H represents an hermitian matrix and M a generic matrix of no symmetry constrains.

As another example, for a 1/2-spin system we have $\mathcal{T} = i\sigma_y \mathcal{K}$ with $\sigma_y = [0 \ -i ; +i \ 0]$ the 2nd Pauli matrix (we reserve σ for Pauli matrices in spin orbital space). In this case $\mathcal{T}^2 = -1$ and $\mathcal{T}\mathcal{H}\mathcal{T}^{-1} = \sigma_y \mathcal{H}^* \sigma_y = \mathcal{H}$ meaning that every energy eigenvalue ε is doubly degenerate. This doubly degeneracy is often refer to as Kramers' degeneracy. In this case, and taking the generic Hamiltonian from Eq.(2), the Hamiltonian would read

$$\mathcal{H} = \left(\begin{array}{c|c} \varepsilon_A \mathbb{1} & M \\ \hline M^\dagger & \varepsilon_B \mathbb{1} \end{array} \right) = \left(\begin{array}{cc|cc} \varepsilon_A & & m_{11} & m_{12} \\ 0 & \varepsilon_A & m_{21} & m_{22} \\ \hline m_{11}^* & m_{21}^* & \varepsilon_B & \\ m_{12}^* & m_{22}^* & 0 & \varepsilon_B \end{array} \right). \quad (3)$$

We can see the consequences of Kramers' degeneracy on the band spectrum versus α in Fig.(1). While the spectrum looks quite similar to the previous ones, whenever a line crosses zero energy, our topological invariant makes a jump of two, and not one. In this case, time-reversal symmetry constrains the topological invariant to only take even values. This is an example of how topological properties can be influenced by discrete symmetries.

4. Sublattice symmetry

We just saw that time-reversal symmetry can forbid the topological invariant to take a certain set of values. We now study another case where a symmetry changes the topological properties dramatically.

Let's now take a system where we can split all the degrees of freedom into two groups—group A and group B —, such that the Hamiltonian only has nonzero matrix elements between two groups, and not inside each group. This situation arises naturally when the a given lattice has two sublattices. For example, for hexagonal boron nitrate (hBN) we can distinguish these sublattices as the boron and nitrogen sites respectively. The matrix of such an Hamiltonian would read

$$\mathcal{H} = \left(\begin{array}{c|c} & M \\ \hline M^\dagger & \end{array} \right) = \left(\begin{array}{cc|cc} 0 & 0 & m_{11} & m_{12} \\ 0 & 0 & m_{21} & m_{22} \\ \hline m_{11}^* & m_{21}^* & 0 & 0 \\ m_{12}^* & m_{22}^* & 0 & 0 \end{array} \right). \quad (4)$$

See that $\eta_z \mathcal{H} \eta_z = -\mathcal{H}$ where $\eta_z = [+1 \ 0 ; 0 \ -1]$ is the 3rd Pauli matrix (we reserve η for Pauli matrices in sublattice orbital space). This immediately means that if $\Psi = [\psi_A ; \psi_B]^T$ is an eigenvector of the Hamiltonian with energy ε , then $[\psi_A ; -\psi_B]^T$ is an eigenvector with energy $-\varepsilon$. A symmetric spectrum is the consequence of sublattice symmetry as seen in Fig.(1). This means that Q always stays constant and that we can always deform Hamiltonians with sublattice symmetry without closing the gap. This indicates that an extra symmetry, such as this one, may render the topology of a system as trivial.

5. Particle-hole symmetry

Another symmetry that has a strong influence on topology is the particle-hole symmetry, showing up in superconducting systems. As we saw in BCS theory, a superconductor will create(annihilate) pairs of electrons by breaking(forming) Cooper pairs costing a pairing energy of Δ to the system.

Let us consider that the dynamics of the electrons is described by the an hermitian H matrix while the pair creation and annihilation is described by an antisymmetric Δ matrix. Understand that

Δ must antisymmetric just because the fermion operators anticommute. The Hamiltonian describing the full system reads

$$\mathcal{H} = \left(\begin{array}{c|c} H & \Delta \\ \hline -\Delta^* & -H^* \end{array} \right) = \left(\begin{array}{cc|cc} h_{11} & h_{12} & 0 & \Delta \\ h_{12}^* & h_{22} & -\Delta & 0 \\ \hline 0 & -\Delta^* & -h_{11}^* & -h_{12}^* \\ \Delta^* & 0 & -h_{12} & -h_{22}^* \end{array} \right) \quad (5)$$

and is known as the Bogoliubov-de Gennes (BdG) Hamiltonian. Moreover, we now double the amount of degrees of freedom in the system by defining a Nambu spinors

$$\check{c}_i^\dagger = \begin{pmatrix} c_i^\dagger & c_i \end{pmatrix} \quad \text{and} \quad \check{c}_i = \begin{pmatrix} c_i \\ c_i^\dagger \end{pmatrix} \quad (6)$$

such that we can write

$$\check{\mathcal{H}} = \frac{1}{2} \check{c}^\dagger \mathcal{H} \check{c}$$

This definition indicates that the Bogoliubov-de Gennes Hamiltonian acts not only on electrons but also on an extra mirror set comprised of electron-holes. Since holes are related to the electrons, \mathcal{H} automatically inherits that extra symmetry. This symmetry exchanges electrons with holes, and has an anti-unitary operator $\mathcal{P} = \tau_x \mathcal{K}$ with $\tau_x = [0 \ 1; 1 \ 0]$ the 1st Pauli matrix (we reserve σ for Pauli matrices in spin orbital space) and (as before) \mathcal{K} complex conjugation. Hence we have that $\mathcal{P}\mathcal{H}\mathcal{P}^{-1} = -\mathcal{H}$. Indeed, for every eigenvector $\Psi = [u; v]^T$ with energy ε , there will be a particle-hole symmetric eigenvector $\mathcal{P}\Psi = [v^*; u^*]^T$ with energy $-\varepsilon$. As clearly seen in Fig.(1), because of the minus sign in the particle-hole symmetry, the spectrum of \mathcal{H} must be mirrored around zero energy, that is, the Fermi level).

Fermionic parity switches See that this spectrum mirroring was also the case for sublattice symmetry however, in this case, energy levels do not repel around zero energy, so that crossings at zero energy appear. Unlike in the case of sublattice symmetry, a pair of $\pm\varepsilon$ energy levels does not correspond to two distinct quantum states, but to a single quantum state. This quantum state is a coherent superposition of electrons and holes, a so called Bogoliubov quasiparticle. It has an excitation energy ε , and it is created by an operator $\gamma^\dagger = uc^\dagger + vc$. Populating the partner state at energy ε is the same as emptying the positive energy state.

In general a crossing between energy levels happens in the presence of a conserved quantity. While the mean-field Hamiltonian of a superconductor does not conserve the number of particles, it conserves the parity of this number. In other words, forming and breaking Cooper pairs does not affect whether the superconducting contains an even or odd number of electrons so fermion parity is a conserved quantity (provided that isolated electrons do not enter or leave the system). Fermion parity, however, is a many-body quantity, which cannot be directly described in terms of the single particle picture of the BdG Hamiltonian. This is why we had to double the number of degrees of freedom by hand. When a pair of levels crosses zero energy, the excitation energy ε of the Bogoliubov quasiparticle changes sign and it becomes favorable to add(remove) a Bogoliubov quasiparticle. In other words, at each crossing the fermion parity in the ground state changes from even to odd (or vice versa), meaning that these crossings are fermion parity switches.

The Pfaffian invariant Since the ground state fermion parity is preserved by the superconducting Hamiltonian if there are no Bogoliubov quasiparticles crossing zero energy, the ground state fermion parity is the topological invariant of this system. It is clear however that this invariant is of a different nature than the one of the non-superconducting systems, which is given by the number Q of negative eigenvalues of the Hamiltonian. The latter cannot change for a BdG Hamiltonian, which has a symmetric energy spectrum, and hence it is not suitable to describe changes in fermion parity. For this

kind of systems the actual topological invariant is called the *Pfaffian*. We will not enter in details on how exactly the Pfaffian is calculated but it will change its value from $Q = +1$ to $Q = 1$ at every zero-energy crossing. You can think of this as if the number of holeonic levels below zero energy counts negatively to the overall positive electronic levels.

B. One-dimensional system

1. Ising model

2. Hubbard model

3. Kitaev model

The most relevant references used for this section follow:

- Kitaev's "Unpaired Majorana fermions in quantum wires" - Phys.-Usp. 44 131
- Akhmerov's "From Kitaev chain to a nanowire" online course - <https://topocondmat.org/>

The *Kitaev chain* or *Kitaev–Majorana chain* is a toy model for a topological superconductor using a 1D hybrid (semiconductor+superconductor) nanowires featuring Majorana bound states.

The Kitaev chain model consists of a 1D linear lattice of N site and spinless fermions at zero temperature, subjected to nearest neighbor hoping interactions. The real-space tight-binding Hamiltonian describing such model reads

$$H = \mu \sum_{i=1}^N \left(c_i^\dagger c_i - \frac{1}{2} \right) - t \sum_{i=1}^{N-1} \left(c_{i+1}^\dagger c_i + h.c. \right) + \Delta \sum_{i=1}^{N-1} \left(c_{i+1}^\dagger c_i^\dagger + h.c. \right) \quad (7)$$

with c_i^\dagger (c_i) fermionic creation (annihilation) operators, μ the chemical potential, t the hopping energy and Δ an proximity induced superconducting p -wave pairing.

The objective of this model definition is to be able to have a Majorana bound states on the edges mode. For this, let us engineering the Hamiltonian in such a special way that it is actually possible to separate two Majoranas. Foremost, we define each site n as if it has two sublattices, $s = A$ and $s = B$. We then define Majorana operators relating to the fermionic operators as

$$\gamma_i^A = c_i^\dagger + c_i \quad \text{and} \quad \gamma_i^B = i (c_i^\dagger - c_i) \quad (8)$$

or rather, in the opposite way, as

$$c_i^\dagger = \frac{1}{2} (\gamma_i^A - i\gamma_i^B) \quad \text{and} \quad c_i = \frac{1}{2} (\gamma_i^A + i\gamma_i^B) \quad (9)$$

Indeed, each site can host a fermion or, equivalently, each site hosting two Majorana modes. These Majorana operators are Hermitian $\gamma_i^s = (\gamma_i^s)^\dagger$, unitary $(\gamma_i^s)^2 = 1$ and anticommute as $\{\gamma_i^s, \gamma_j^{s'}\} = 2\delta_{ij}\delta_{ss'}$.

Substituting directly into the Hamiltonian of Eq.(7) the fermionic operators as given by Eqs.(9) we obtain

$$H = -i\mu \frac{1}{2} \sum_{i=1}^N \gamma_i^B \gamma_i^A + i \frac{1}{2} \sum_{i=1}^{N-1} (\omega_+ \gamma_i^B \gamma_{i+1}^A + \omega_- \gamma_{i+1}^B \gamma_i^A), \quad \text{with } \omega_\pm = \Delta \pm t \quad (10)$$

From it we can distinguish between two phases—trivial and topological—, corresponding, respectively, to two different ways of pairing these Majoranas states—no unpaired modes or one isolated mode on both edges. These pairing configuration are depicted in Fig.2 in blue and red respectively. This phases can be easily identified, respectively, in their limiting regimes where one sets $\Delta = t = 0$ and $\mu = 0$ with $\Delta = t \neq 0$.



Figure 2. Kitaev chain Majorana modes pairing possibilities

Indeed, see that by setting $\Delta = t = 0$ within the Hamiltonian of Eq.(10) we obtain

$$H_{\text{trivial}} = -i\mu \frac{1}{2} \sum_{i=1}^N \gamma_i^B \gamma_i^A, \quad (11)$$

which corresponds to the limiting case of "no unpaired Majorana modes" configuration. The energy cost for each fermion to be occupied is μ , with all excitations having an energy of either $\pm\mu/2$. The band structure will then have a gapped bulk and no zero energy edge states. Furthermore, see that the wavefunctions of the first three energy states shown in Fig.(3).(middle) in this trivial phase simply resemble the harmonic modes of a string states.

On the other hand, see that by setting $\mu = 0$ with $\Delta = t \neq 0$ we obtain

$$H_{\text{topological}} = it \sum_{n=1}^{N-1} \gamma_n^B \gamma_{n+1}^A \quad (12)$$

which corresponds to the "unpaired edge Majorana mode" configuration where every Majorana operator is coupled to a Majorana operator of a different kind in the next site. Note that the summation only goes up to $n = N - 1$. Moreover, see that by assigning a new fermion operator $\tilde{c}_i = 1/2 (\gamma_i^B + i\gamma_{i+1}^A)$, the Hamiltonian can be otherwise expressed as

$$H_{\text{topological}} = 2t \sum_{n=1}^{N-1} \left(\tilde{c}_n^\dagger \tilde{c}_n + \frac{1}{2} \right) \quad (13)$$

which describes a new set of $N - 1$ Bogoliubov quasiparticles with energy t . For every Majorana pair we assign an energy difference $2t$ between the empty and filled state. All states which are not at the ends of the chain have an energy of $\pm t$ and thus the bands structure has a gapped bulk. However, see that the missing mode $\tilde{c}_N = 1/2 (\gamma_N^B + i\gamma_1^A)$, which couples the Majorana operators from the two endpoints of the chain, does not appear in the Hamiltonian and thus it most have zero energy. As the presence of this mode does not change the total energy, the ground state is two-fold degenerate. This condition is a topological superconducting non-trivial phase. This mode is called a Majorana zero mode and is highly delocalized at the edges, as it can be seen in red in Fig(3).(middle). As one tunes μ in the direction of the trivial phase, the topological gap, protected by particle-hole symmetry (PHS), gets smaller and smaller and the Majoranas wavefunctions stay less and less localized at the edges. At the transition between the trivial and topological, when the chemical potential takes it's critical value of $|\mu| = 2t$, the first energy states stays evenly distributed along the chain.

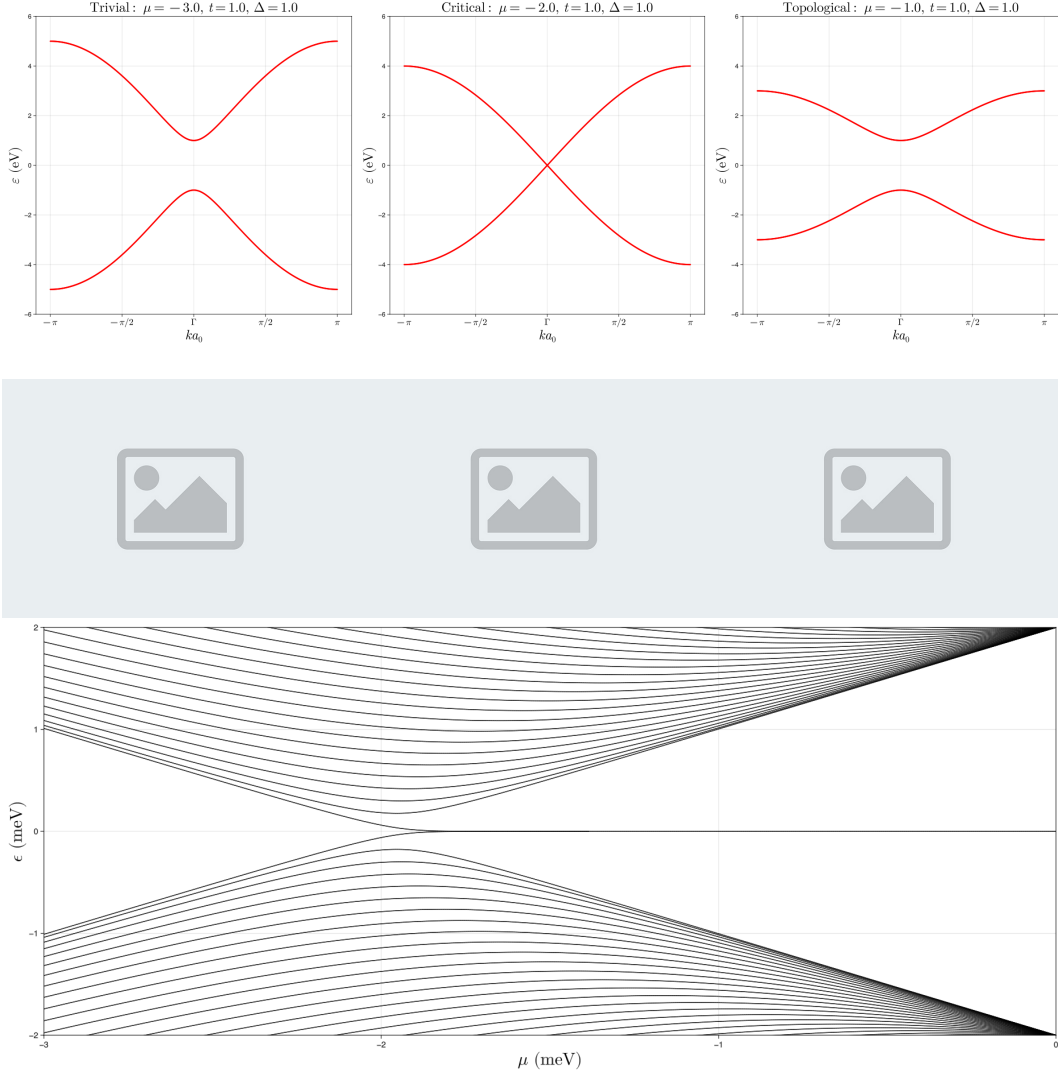


Figure 3. Kitaev chain (top) band structure (middle) I will eventually plot the 1st, 2nd and 3rd state wavefunction here at each regime, and (bottom) band spectrum for a chain length of $L = 50$ with lattice spacing $a_0 = 1$ fixing $\Delta = t = 1.0$. The critical μ shifts forward to infinity as $L \rightarrow 0$.

Majorana modes at a domain wall Consider the case where we weld together two semi-infinite nanowires with one in it's trivial phase and the other in it's trivial phase. The spacial profile of the chemical potential $\mu(x)$ would then approximately a Heaviside theta function from $|\mu_{\text{left}}| > 2t$ to $|\mu_{\text{right}}| < 2t$, forming a doping domain wall at it's center. Hamiltonian wise, one just substitutes $\mu \rightarrow \mu(x)$ directly into Eq.(7). What one obtains in this situation is a Majorana mode localized at the domain wall with its twin forming in the semi-infinite edge of the topological side.

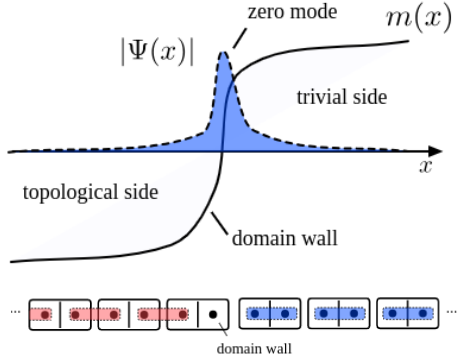


Figure 4. needs caption

Bogoliubov-de Gennes Hamiltonian Let us now define the Hamiltonian in Eq.(7) in its Bogoliubov-de Gennes (BdG) form

$$H = \frac{1}{2} \check{c}^\dagger H_{\text{BdG}} \check{c}.$$

where we have defined the Nambu spinor as

$$\check{c}_i^\dagger = \begin{pmatrix} c_i^\dagger & c_i \end{pmatrix} \quad \text{and} \quad \check{c}_i = \begin{pmatrix} c_i \\ c_i^\dagger \end{pmatrix} \quad (14)$$

This proves not only useful to the study of the system's symmetries, but it also a necessary step for the numerical implementation in *Quantical.jl*. Defining τ_x, τ_y, τ_z as Pauli matrices in the particle-hole subspace and using the fermionic anti-commutation properties $\{c_i, c_j^\dagger\} = \delta_{ij}$ and $\{c_i, c_j\} = 0$, one can check that

$$\mu : \quad \check{c}_i^\dagger \tau_z \check{c}_i = \begin{pmatrix} c_i^\dagger & c_i \end{pmatrix} \begin{pmatrix} 1 & 0 \\ 0 & -1 \end{pmatrix} \begin{pmatrix} c_i \\ c_i^\dagger \end{pmatrix} = c_i^\dagger c_i - c_i c_i^\dagger = 2c_i^\dagger c_i - 1 \quad (15)$$

$$t : \quad \check{c}_j^\dagger \tau_z \check{c}_i = \begin{pmatrix} c_j^\dagger & c_j \end{pmatrix} \begin{pmatrix} 1 & 0 \\ 0 & -1 \end{pmatrix} \begin{pmatrix} c_i \\ c_i^\dagger \end{pmatrix} = c_j^\dagger c_i - c_j c_i^\dagger = c_j^\dagger c_i + h.c \quad (16)$$

$$\Delta : \quad \check{c}_j^\dagger i \tau_y \check{c}_i = \begin{pmatrix} c_j^\dagger & c_j \end{pmatrix} \begin{pmatrix} 0 & 1 \\ -1 & 0 \end{pmatrix} \begin{pmatrix} c_i \\ c_i^\dagger \end{pmatrix} = c_j^\dagger c_i^\dagger - c_j c_i = c_j^\dagger c_i^\dagger + h.c \quad (17)$$

Hence the Hamiltonian in Eq.(7) in its BdG form reads as

$$H = \mu \frac{1}{2} \sum_i \check{c}_i^\dagger \tau_z \check{c}_i - t \sum_{i=1}^{N-1} \check{c}_{i+1}^\dagger \tau_z \check{c}_i + \Delta \sum_{i=1}^{N-1} \check{c}_{i+1}^\dagger i \tau_y \check{c}_i \quad (18)$$

See that the Hamiltonian has particle-hole symmetry, i.e. $\mathcal{P}H\mathcal{P}^{-1} = -\tau_x H^* \tau_x = -H$ with $\mathcal{P} = \tau_x \mathcal{K}$ and \mathcal{K} complex conjugation, as well as time reversal symmetry, i.e. $\mathcal{T}H\mathcal{T}^{-1} = H^* = H$ with $\mathcal{T} = \mathcal{K}$ for this spinless case (for reference, $\mathcal{T} = i\sigma_y \mathcal{K}$ for a 1/2-spin system). Once again, to understand why this is the case check.

Topological invariant We will not attempt to give a rigorous derivation of the bulk invariant - a task which is often difficult even for advanced researchers in the field - but rather to arrive at it in a heuristic manner.

We can start with some important clues. On the one hand, we are studying a Bogoliubov-de Gennes Hamiltonian, and we have already learned that quantum dots with particle-hole symmetry are characterized by a topological invariant, the sign of the Pfaffian, which changes sign at every gap closing. On the other hand, we have just seen that the gap closing in the Kitaev chain model is accompanied by a change of sign of m . This suggests to try to link the quantity m to a Pfaffian. How to do so?

In fact, you can think of the full *HBdG* as a very large matrix with particle-hole symmetry. It can be put in antisymmetric form and we can compute its Pfaffian. This Pfaffian may change only when an eigenvalue of $H(k)$ passes through zero. Because of particle-hole symmetry, for every eigenvalue $E(k)$ we have one at $-E(-k)$. So if $E(k)$ passes through zero, also its partner does. Furthermore, the spectrum has to be periodic in the Brillouin zone, which means that gap closings at finite momentum always come in pairs, and cannot change the Pfaffian. There are only two points which make exception: $k=0$ and $k=\pi$, which are mapped onto themselves by particle-hole symmetry. In fact, for these points we have:

4. *SSH model*

The most relevant references used for this section follow:

- Asboth's "A short course on topological insulators" - arXiv:1509.02295..

5. *Oreg-Lutchyn model*

The most relevant references used for this section follow:

- Lutchyn's "Majorana Fermions and a Topological Phase Transition in Semiconductor-Superconductor Heterostructures "- Phys. Rev. Lett. 105, 077001
- Oreg's "Helical liquids and Majorana bound states in quantum wires" - Phys. Rev. Lett. 105, 177002
- Lobo's "Exponential suppression of the topological gap in self-consistent intrinsic Majorana nanowires" - arXiv:2412.15174

The Oreg-Lutchyn Majorana minimal model consists of a finite 1D semiconductor (SM) nanowire with strong spin-orbit coupling (SOC) α and a tunable chemical potential μ , in proximity of a superconductor (SC) of homogeneous pairing Δ , having a magnetic field B_z applied along its length, defined as the \hat{z} direction. The Rashba effect describes the coupling of an electric field E_x that breaks inversion symmetry breaking in the direction perpendicular to the wire, to the electron's spin, i.e $\propto (i\vec{\nabla} \times \hat{x}) \cdot \vec{\sigma} = i\sigma_y \partial_z$ with $\vec{\sigma} = (\sigma_x, \sigma_y, \sigma_z)$. The Zeeman effect described the spin splitting due to the in-plane magnetic field B_z . The pairing term describes the Cooper pairs from BCS theory than could tunnel from the SM to the SC.

The tight-binding Hamiltonian describing such system can then be decomposed as

$$H = H_K + H_{SOC} + H_Z + H_{SC} \quad (19)$$

$$H_K = (2t - \mu) \sum_{i\sigma} c_{i\sigma}^\dagger c_{i\sigma} - t \sum_{\langle i,j \rangle \sigma} c_{i\sigma}^\dagger c_{j\sigma} \quad (20)$$

$$H_{SOC} = \frac{\alpha}{2a_0} \sum_{i\sigma} (c_{i+1\bar{\sigma}}^\dagger c_{i\sigma} + h.c.) \quad (21)$$

$$H_Z = V_Z \sum_i (c_{i\uparrow}^\dagger c_{i\uparrow} - c_{i\downarrow}^\dagger c_{i\downarrow}) \quad (22)$$

$$H_{SC} = \Delta (c_{i\downarrow}^\dagger c_{i\uparrow}^\dagger + h.c.) \quad (23)$$

with c_i^\dagger (c_i) fermionic creation (annihilation) operators, μ the chemical potential, $t = \eta/a_0^2$ the hopping energy into $\langle i, j \rangle$ nearest-neighbouring sites with a_0 the lattice constant and $\eta = \hbar^2/2m^*$ with m^* the effective mass of the electrons, $V_Z = g_J \mu_B B_z/2$ the Zeeman potential with g_J the Landé gyromagnetic moment and μ_B Bohr's magneton, α the Rashba SOC strength and Δ proximity induced superconducting s -wave pairing.

A paragraph explaining the bands.

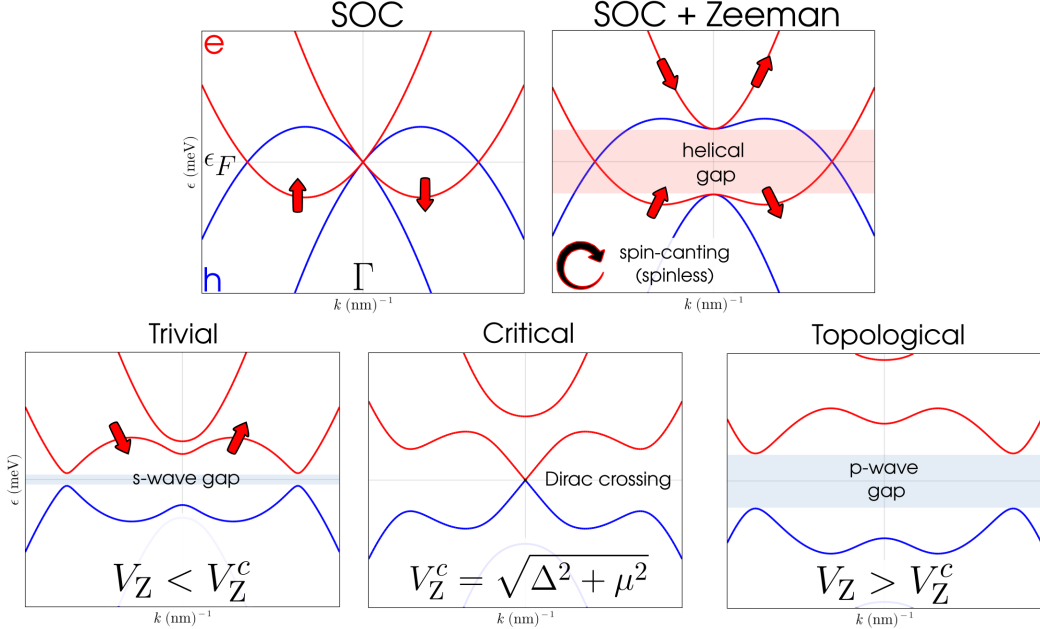


Figure 5.

A paragraph explaining the phase-diagram, pfaffian and band spectrum.

Numerical implementation in Quantica.jl Shown below are the broad strokes of a numerical implementation of the Hamiltonian in Julia using the Quantica.jl. However, prior to this implementation, we will be needing the Bogoliubov-de Gennes formalism. For this, need to double the degrees of freedom through the Nambu-spinor. In the so called unrotated-spin basis we define a Nambu spinor as

$$\check{c}_i^\dagger = \begin{pmatrix} c_i^\dagger & c_i \end{pmatrix} = \begin{pmatrix} c_{i\uparrow}^\dagger & c_{i\downarrow}^\dagger & c_{i\uparrow} & c_{i\downarrow} \end{pmatrix} \quad (24)$$

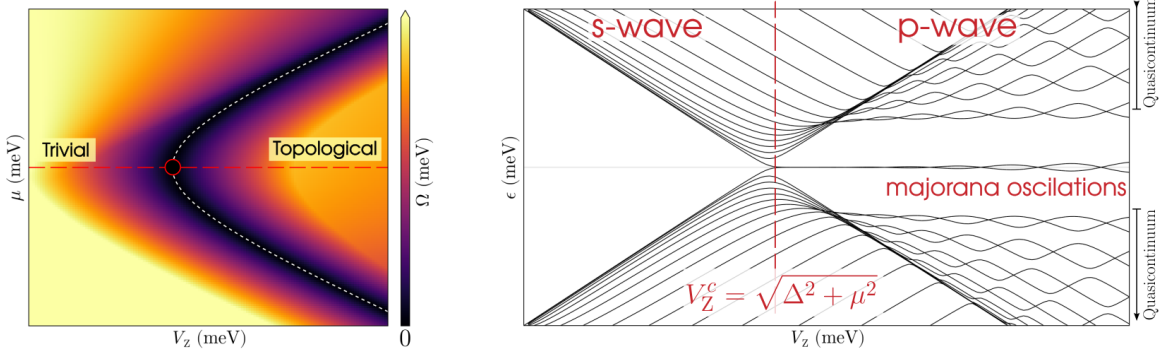


Figure 6.

In this Nambu \otimes spin orbital space the Hamiltonian in Eq.(19) reads

$$H = H_K + H_{\text{SOC}} + H_Z + H_{\text{SC}} \quad (25)$$

$$H_K = (2t - \mu) \sum_i \check{c}_i^\dagger [\tau_z \otimes \sigma_0] \check{c}_i - \frac{1}{2} t \sum_{\langle i,j \rangle} \check{c}_i^\dagger [\tau_z \otimes \sigma_0] \check{c}_j \quad (26)$$

$$H_{\text{SOC}} = \frac{\alpha}{2a_0} \sum_i \check{c}_i^\dagger [\tau_z \otimes i\sigma_y] \check{c}_{i+1} \quad (27)$$

$$H_Z = V_Z \sum_i \check{c}_i^\dagger [\tau_z \otimes \sigma_z] \check{c}_i \quad (28)$$

$$H_{\text{SC}} = \frac{1}{2} \Delta \sum_i \check{c}_i^\dagger [\tau_y \otimes \sigma_y] \check{c}_i \quad (29)$$

with τ Pauli matrices in the particle-hole subspace and σ in the spin subspace.

To understand why this is the case check we show explicitly the derivation for the pairing term as an example. It reads:

$$\begin{aligned} \check{c}^\dagger [\tau_y \otimes \sigma_y] \check{c} &= \left(\begin{array}{ccc} c_\uparrow^\dagger & c_\downarrow^\dagger & c_\uparrow & c_\downarrow \end{array} \right) \left(\begin{array}{cc|cc} 0 & 0 & 0 & -1 \\ 0 & 0 & +1 & 0 \\ \hline 0 & +1 & 0 & 0 \\ -1 & 0 & 0 & 0 \end{array} \right) \left(\begin{array}{c} c_\uparrow \\ c_\downarrow \\ c_\uparrow^\dagger \\ c_\downarrow^\dagger \end{array} \right) \\ &= -c_\uparrow^\dagger c_\downarrow^\dagger + c_\downarrow^\dagger c_\uparrow^\dagger + c_\uparrow c_\downarrow - c_\downarrow c_\uparrow = 2 \left(c_\downarrow^\dagger c_\uparrow^\dagger + \text{h.c.} \right) \end{aligned} \quad (30)$$

where we the fermionic anti-commutation properties $\{c_i, c_j^\dagger\} = \delta_{ij}$ and $\{c_i, c_j\} = 0$.

The remaining terms derivation is analogous but even simpler because there is will be no mixing of particle with particle-hole components; the holeonic terms will correspond to the negative of the electronic terms, meaning that one just needs to expand the space according to $\tau_z \otimes$ the respective spin matrix. For the kinetic term there is no mixing of spin so it must trivially have the spin Pauli matrix σ_0 . Similarly, for the Zeeman term there is only the same-spin mixing of the type $\uparrow\uparrow - \downarrow\downarrow$ so it must have σ_z . As for the SOC term there is spin-mixing of opposing spins, so the options are either σ_x or $i\sigma_y$ (with a i for it to be hermitian). One can check with the fermionic anti-commutation properties that it is indeed $i\sigma_y$.

Alternative Nambu basis It is common for people to define instead the Nambu spinor in a rotated basis as such

$$\bar{\mathbf{c}}_i^\dagger = \left(\begin{array}{cc} \mathbf{c}_i^\dagger & [i\sigma_y \mathbf{c}_i] \end{array} \right) = \left(\begin{array}{cc|cc} c_{i\uparrow}^\dagger & c_{i\downarrow}^\dagger & c_{i\downarrow} & -c_{i\uparrow} \end{array} \right) \quad (31)$$

As also explained in section II.C.1 of the previous part, these basis' operators relate to each other as

$$\bar{\mathbf{c}}_i = \bar{\mathcal{U}} \check{\mathbf{c}}_i \Leftrightarrow \check{\mathbf{c}}_i = \bar{\mathcal{U}}^\dagger \bar{\mathbf{c}}_i \quad (32)$$

$$\bar{\mathbf{c}}_i^\dagger = \check{\mathbf{c}}_i^\dagger \bar{\mathcal{U}}^\dagger \Leftrightarrow \check{\mathbf{c}}_i^\dagger = \bar{\mathbf{c}}_i^\dagger \bar{\mathcal{U}} \quad (33)$$

and, consequently, for a generic $\check{\mathbf{M}}$ matrix,

$$\bar{\mathbf{M}} = \bar{\mathcal{U}} \check{\mathbf{M}} \bar{\mathcal{U}}^\dagger \quad (34)$$

with $\bar{\mathcal{U}}$ is a unitary matrix (i.e $\bar{\mathcal{U}}^\dagger \bar{\mathcal{U}} = \bar{\mathcal{U}} \bar{\mathcal{U}}^\dagger = \mathbb{1}$)

$$\bar{\mathcal{U}} = \begin{pmatrix} \sigma_0 & 0 \\ 0 & i\sigma_y \end{pmatrix} \quad (35)$$

Making use of Pauli matrices' property

$$\sigma_\alpha \sigma_\beta = \sigma = \sigma_0 \delta_{\alpha\beta} + i\varepsilon_{\alpha\beta\gamma} \sigma_\gamma \quad (36)$$

one can check that

$$H_K : \bar{\mathcal{U}} [\tau_z \otimes \sigma_0] \bar{\mathcal{U}}^\dagger = [\tau_z \otimes \sigma_0] \quad (37)$$

$$H_{SOC} : \bar{\mathcal{U}} [\tau_z \otimes i\sigma_y] \bar{\mathcal{U}}^\dagger = [\tau_z \otimes i\sigma_y] \quad (38)$$

$$H_Z : \bar{\mathcal{U}} [\tau_z \otimes \sigma_z] \bar{\mathcal{U}}^\dagger = [\tau_z \otimes \sigma_z] \quad (39)$$

$$H_{SC} : \bar{\mathcal{U}} [\tau_y \otimes \sigma_y] \bar{\mathcal{U}}^\dagger = [\tau_x \otimes \sigma_0] \quad (40)$$

meaning that, in this the rotated basis, only the pairing Hamiltonian has it's Pauli matrices changed. Concretely,

$$H_{SC} = \frac{1}{2} \Delta \sum_i \bar{\mathbf{c}}_i^\dagger [\tau_x \otimes \sigma_0] \bar{\mathbf{c}}_i \quad (41)$$

C. Hall effects

1. Integer quantum Hall effect
2. Quantum spin Hall (Kane-Mele) effect
3. Quantum anomalous Hall effect
4. Fraction Hall effect

D. Graphene

1. Monolayer graphene

Hexagonal boron nitride (hBN) is a 2D material composed of a simple layer of alternating boron and nitrogen atoms disposed in a planar honeycomb lattice, as shown in Fig.(8)(a). The Bravais lattice

$$\mathbf{r}_i = n_{i1}\mathbf{a}_1 + n_{i2}\mathbf{a}_2, \quad n_{i1}, n_{i2} \in \mathbb{Z} \quad (42)$$

is generated by the real vectors basis

$$\mathbf{a}_1 = a_0 \begin{bmatrix} +\sin(30^\circ) \\ +\cos(30^\circ) \end{bmatrix} \text{ and } \mathbf{a}_2 = a_0 \begin{bmatrix} +\sin(30^\circ) \\ -\cos(30^\circ) \end{bmatrix}. \quad (43)$$

where $\sin(30^\circ) = 1/2$ and $\cos(30^\circ) = \sqrt{3}/2$. In each diamond shaped Wigner-Seitz primitive cell (depicted in yellow), we have one boron atom and one nitride atom, which we designate as sub-lattices *A* (depicted in red) and *B* (depicted in blue) respectively. The atoms within the central primitive cell are located at

$$\mathbf{s}_A = \frac{a_0}{\sqrt{3}} \begin{bmatrix} 0 \\ -1/2 \end{bmatrix} \text{ and } \mathbf{s}_B = \frac{a_0}{\sqrt{3}} \begin{bmatrix} 0 \\ +1/2 \end{bmatrix}. \quad (44)$$

where the origin is defined at the midpoint between the atoms. For each site *A*, the position of the nearest-neighbors (NN) in the sites *B* are given by

$$\boldsymbol{\delta}_1 = \frac{a_0}{\sqrt{3}} \begin{bmatrix} 0 \\ 1 \end{bmatrix}, \quad \boldsymbol{\delta}_2 = \frac{a_0}{\sqrt{3}} \begin{bmatrix} +\sin(60^\circ) \\ -\cos(60^\circ) \end{bmatrix} \text{ and } \boldsymbol{\delta}_3 = \frac{a_0}{\sqrt{3}} \begin{bmatrix} -\sin(60^\circ) \\ -\cos(60^\circ) \end{bmatrix}. \quad (45)$$

where $\sin(60^\circ) = \sqrt{3}/2$ and $\cos(60^\circ) = 1/2$. All these vectors are shown in Fig.(8)(a) within the real space lattice. Furthermore, from the real lattice basis vectors, in order to fulfill $\mathbf{a}_i \cdot \mathbf{b}_j = 2\pi\delta_{ij}$, the reciprocal lattice basis vectors follow as

$$\mathbf{b}_1 = \frac{2\pi}{a_0} \begin{bmatrix} +\cos(30^\circ) \\ -\sin(30^\circ) \end{bmatrix} \text{ and } \mathbf{b}_2 = \frac{2\pi}{a_0} \begin{bmatrix} +\cos(30^\circ) \\ +\sin(30^\circ) \end{bmatrix}. \quad (46)$$

These are also shown in Fig.(8)(b) together with the first zone of Brillouin, formed by the area enclosed by the intersection of their bisectrices. The high-symmetry points are Γ , the origin, the Dirac points K_\pm and M read as

$$\boldsymbol{\Gamma} = \begin{bmatrix} 0 \\ 0 \end{bmatrix}, \quad K_\pm = \pm \frac{4\pi}{3a_0} \begin{bmatrix} 1 \\ 0 \end{bmatrix} \text{ and } M = \frac{2\pi}{a_0} \begin{bmatrix} +\cos(30^\circ)/2 \\ +\sin(30^\circ)/2 \end{bmatrix} \quad (47)$$

where the K point is found such that $(\mathbf{M} + K_{k_x} \hat{\mathbf{M}}_\perp)_{k_y} = 0$, with $\hat{\mathbf{M}}_\perp$ the unit vector in the perpendicular direction to \mathbf{M} . In far right side of Fig.(7), we make a note that the discretized grid it's in the Bloch momentums basis $\{\phi_1, \phi_2\}$, i.e in the direction of the reciprocal lattice vectors, and not simply in the reciprocal space $\{k_x, k_y\}$. In the Bloch momentums basis the Dirac points would reads as $K_\pm = 2\pi/3a_0 [\pm 1, \mp 1]$.

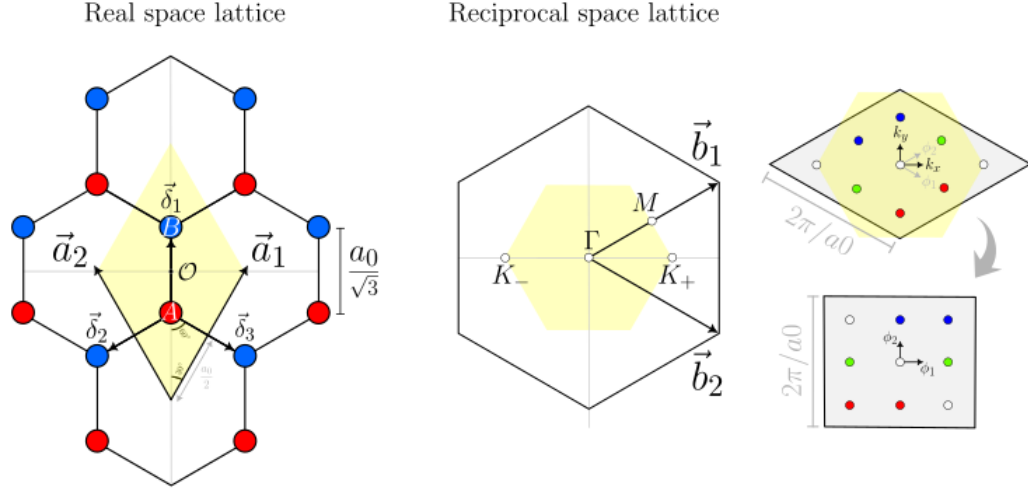


Figure 7.

Let us consider the nearest-neighbors (NN) tight-binding model, written in real space as

$$H_{\text{TB}}(\mathbf{R}) = \sum_i \epsilon_A a_{\mathbf{r}_i}^\dagger a_{\mathbf{r}_i} + \sum_i \epsilon_B b_{\mathbf{r}_i}^\dagger b_{\mathbf{r}_i} - t \sum_{\langle i,j \rangle} (a_{\mathbf{r}_i}^\dagger b_{\mathbf{r}_i+\delta_j} + b_{\mathbf{r}_j}^\dagger a_{\mathbf{r}_i-\delta_j}), \quad (48)$$

where the operators $a_{\mathbf{r}_i}^\dagger (a_{\mathbf{r}_i})$ create (annihilate) an electron in the sub-lattice A in a given Bravais lattice site \mathbf{r}_i , the operators $b_{\mathbf{r}_i}^\dagger (b_{\mathbf{r}_i})$ the same but for sub-lattice B , ϵ_A and ϵ_B are the onsite energies of site A and B respectively, and t is the hopping strength between nearest-neighbouring sites A and B and back, denoted with $\langle i,j \rangle$.

Expressing the creation/annihilation operators as their Fourier counterparts,

$$a_{\mathbf{R}_i} = \frac{1}{\sqrt{V}} \sum_{\mathbf{k}} e^{+i\mathbf{k}\cdot(\mathbf{R}_i+\mathbf{s}_A)} a_{\mathbf{k}} \quad \text{and} \quad b_{\mathbf{R}_i} = \frac{1}{\sqrt{V}} \sum_{\mathbf{k}} e^{+i\mathbf{k}\cdot(\mathbf{R}_i+\mathbf{s}_B)} b_{\mathbf{k}}, \quad (49)$$

and using the identity $\delta(\mathbf{k} - \mathbf{k}') = 1/N \sum_i e^{-i\mathbf{R}_i \cdot (\mathbf{k} - \mathbf{k}')}$, we obtain the Hamiltonian in reciprocal space,

$$H_{\text{TB}}(\mathbf{R}) = \sum_{\mathbf{k}} \epsilon_A a_{\mathbf{k}}^\dagger a_{\mathbf{k}} + \sum_{\mathbf{k}} \epsilon_B b_{\mathbf{k}}^\dagger b_{\mathbf{k}} - t \sum_{\mathbf{k}} (\gamma_{\mathbf{k}} a_{\mathbf{k}}^\dagger b_{\mathbf{k}} + \gamma_{\mathbf{k}}^\dagger b_{\mathbf{k}}^\dagger a_{\mathbf{k}}), \quad (50)$$

where $\gamma_{\mathbf{k}} = \sum_{\langle j \rangle} \exp(+i\mathbf{k} \cdot \delta_j)$ is complex number. If we now define a row vector $c_{\mathbf{k}}^\dagger = [a_{\mathbf{k}}^\dagger \ b_{\mathbf{k}}^\dagger]$ we can rewrite the system's Hamiltonian as $H_{\mathbf{R}}^{\text{TB}} = \sum_{\mathbf{k}} c_{\mathbf{k}}^\dagger H_{\mathbf{k}}^{\text{TB}} c_{\mathbf{k}}$ with

$$H_{\text{TB}}(\mathbf{k}) = \begin{bmatrix} \epsilon_A & -t\gamma_{\mathbf{k}} \\ -t\gamma_{\mathbf{k}}^\dagger & \epsilon_B \end{bmatrix}. \quad (51)$$

Within this simplified tight-binding model, the expression for the electronic two-band structure can easily be obtained analytically by diagonalizing the matrix in Eq.(51), yielding

$$E_{\text{TB}}^{\pm}(\mathbf{k}) = \pm \sqrt{\epsilon^2 + t^2 \left[3 + 2 \cos(a_0 k_x) + 4 \cos\left(\frac{a_0 \sqrt{3}}{2} k_y\right) \cos\left(\frac{a_0}{2} k_x\right) \right]}, \quad (52)$$

having defined the zero point energy at $(\epsilon_A + \epsilon_B)/2$ and defined $\epsilon \equiv (\epsilon_A - \epsilon_B)/2$ at the middle of the gap such that $\epsilon_A = \epsilon$ and $\epsilon_B = -\epsilon$. The valence band corresponds to the $E_{\text{TB}}^-(\mathbf{k})$ dispersion while the $E_{\text{TB}}^+(\mathbf{k})$ corresponds to the conduction band, as shown in Fig.(8)(c). The band structure is accompanied by the density of states $\text{DoS}(E) = \sum_{\mathbf{k}} \delta(E - E(\mathbf{k}))$.

Notice that, if $\epsilon_A = \epsilon_B$, as is the case for graphene, we obtain $\epsilon = 0$ and the band dispersion closes in a linear fashion at the so called Dirac points. In hBN, the electronic band dispersion is also at its minimum near these points but has instead a parabolic shape. In either case, these points represent a fundamental symmetry of the system, called valley parity. To see why the dispersion is parabolic at these valley points, we Taylor series expand the exponential of $\gamma_{\mathbf{k}}$ in Eq.(??) near $\mathbf{k} \rightarrow \mathbf{K} + \mathbf{p}$ with $\mathbf{p} \rightarrow 0$. We obtain $\exp(+i\mathbf{p} \cdot \boldsymbol{\delta}_j) \approx 1 + i\mathbf{p} \cdot \boldsymbol{\delta}_j$. Now, since $\sum_{\langle j \rangle} \exp(+i\mathbf{K} \cdot \boldsymbol{\delta}_j) = 0$ we are left with $\gamma_{\mathbf{K} + \mathbf{p}} \simeq i\mathbf{p} \cdot \sum_{\langle j \rangle} \exp(+i\mathbf{K} \cdot \boldsymbol{\delta}_j) \boldsymbol{\delta}_j = -\sqrt{3}a_0/2(p_x - ip_y)$. Invoking the Pauli matrices definitions, from Eq.(51) we can write the TB Hamiltonian $H_{\text{TB}}^{\mathbf{k}}$ in this low-energy regime as

$$H_{\text{TB}}(\mathbf{K} + \mathbf{p}) = \epsilon \sigma_z + t \frac{\sqrt{3}a_0}{2} (\mathbf{p} \cdot \boldsymbol{\sigma}), \quad (53)$$

which clearly resembles the 2D Dirac Hamiltonian, $H_{\text{Dirac}} = \sigma_z mc^2 + c(\mathbf{p} \cdot \boldsymbol{\sigma})$ with ϵ taking the role of the rest mass energy mc^2 and instead with a velocity $v_F = t\sqrt{3}a_0/2$, termed the *Fermi velocity*, as a replacement to the velocity of light c . Notice that, for the case of graphene, since $\epsilon = 0$, the electrons would behave as if they are massless. In this limit, the hBN low-energy dispersion can be written as the typical relativistic dispersion relation

$$E_{\text{TB}}(\mathbf{K} + \mathbf{p}) = \pm \sqrt{p^2 v_F^2 + m_{\text{eff}}^2 v_F^4}. \quad (54)$$

where m_{eff} is the effective mass of the electron at a given point near the valleys.

Refazer esta figura em Quantica para aprender a fazer densidade de estados. Falar das singularidades de van Hove.

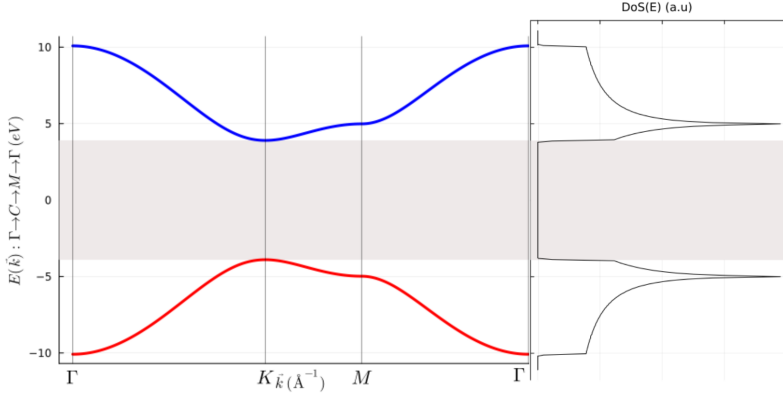


Figure 8. hBN electronic band structure from a nearest-neighbor tight-binding model accompanied by the density of the states. The dispersion goes along the symmetry path $\mathbf{k} : \Gamma \rightarrow K \rightarrow M \rightarrow \Gamma$ and was calculated using $\epsilon_g = 7.8\text{eV}$ for the energy gap, $t = 3.1\text{eV}$ for the hopping parameter and $a_0 = 1.42\sqrt{3}\text{\AA}$ for the honeycomb lattice length.

2. Bilayer Bernal graphene

Consider a bilayer graphene model depicted in Fig.(9).

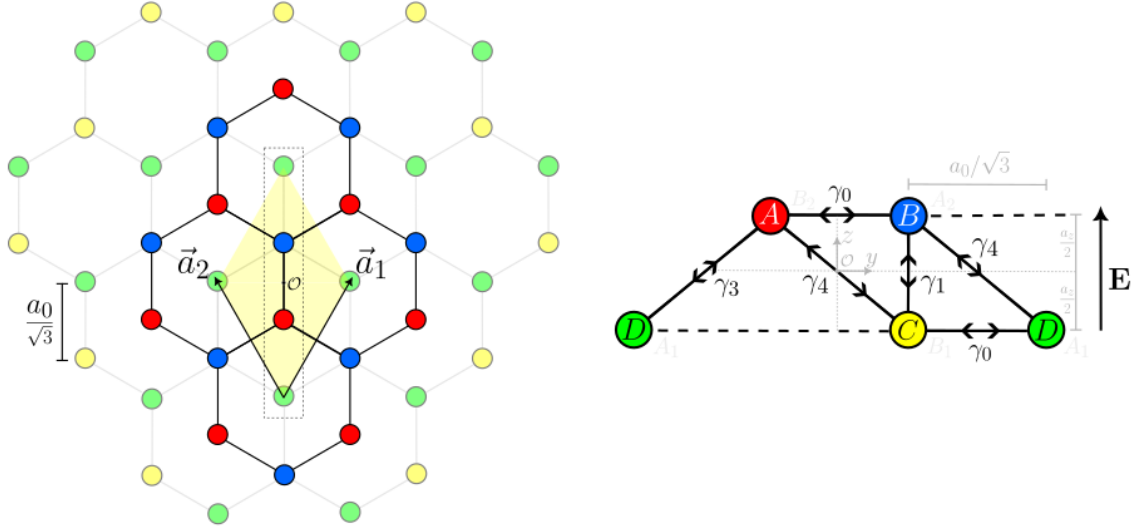


Figure 9. (a) Top view of the bilayer graphene (b) Side view of the dotted region in (a)

The tight-binding Hamiltonian of such a model reads

$$\begin{aligned}
H_{\text{BLG}} &= H_{\text{intralayer}} + H_{\text{interlayer}} = (H_{\text{top}} + H_{\text{bot}}) + (H_{\gamma_1} + H_{\gamma_3} + H_{\gamma_4}) \\
H_{\text{top}} &= \sum_i (\epsilon_A - \mu) c_i^\dagger a_i + \sum_i (\epsilon_B - \mu) b_i^\dagger b_i - \gamma_0 \sum_{\langle i,j \rangle} (a_i^\dagger b_j + h.c.) \\
H_{\text{bot}} &= \sum_i (\epsilon_C - \mu) c_i^\dagger c_i + \sum_i (\epsilon_D - \mu) d_i^\dagger d_i - \gamma_0 \sum_{\langle i,j \rangle} (c_i^\dagger d_j + h.c.) \\
H_{\gamma_1} &= +\gamma_1 \sum_{\langle i,j \rangle} (b_i^\dagger c_j + h.c.) \\
H_{\gamma_3} &= -\gamma_3 \sum_{\langle i,j \rangle} (a_i^\dagger d_j + h.c.) \\
H_{\gamma_4} &= +\gamma_4 \sum_{\langle i,j \rangle} (b_i^\dagger d_j + h.c.) + t_4 \sum_{\langle i,j \rangle} (a_i^\dagger C_j + h.c.)
\end{aligned}$$

Here, a site located at \mathbf{r}_i is indexed by the side index i and its next nearest neighbors located at \mathbf{r}_j are indexed with the site index j . Of course, \mathbf{r}_j depends on the kind of hopping in questions: for γ_0 it's $\mathbf{r}_j = \mathbf{r}_i + \boldsymbol{\delta}_j$ with $j = 1, 2, 3$, for γ_1 it's $\mathbf{r}_j = \mathbf{r}_i \pm a_z \hat{\mathbf{z}}$, and for γ_3 and γ_4 it's $\mathbf{r}_j = \mathbf{r}_i + \boldsymbol{\delta}_j \pm a_z \hat{\mathbf{z}}$. Moreover, let us consider an electric field \mathbf{E} uniform in the plane xOy and growing along the $\hat{\mathbf{z}}$, described by the tight-binding Hamiltonian

$$H_E = \sum_i E_i (f_{i\uparrow}^\dagger f_{i\uparrow} - f_{i\downarrow}^\dagger f_{i\downarrow})$$

where $E_i = E \times z_i$ is the amplitude of the electric field at position \mathbf{r}_i , only really dependent on z_i , and $f_i^\dagger = [f_{i\uparrow}^\dagger \ f_{i\downarrow}^\dagger]$ is a generic fermionic operator. Since in our bilayer model the bottom layer is situated at $z = 0$ we redefine $E(a_z) = E$, such that

$$H_{\text{BLG}+} = E \sum_i \left\{ (a_{i\uparrow}^\dagger a_{i\uparrow} - a_{i\downarrow}^\dagger a_{i\downarrow}) + (b_{i\uparrow}^\dagger b_{i\uparrow} - b_{i\downarrow}^\dagger b_{i\downarrow}) \right\}$$

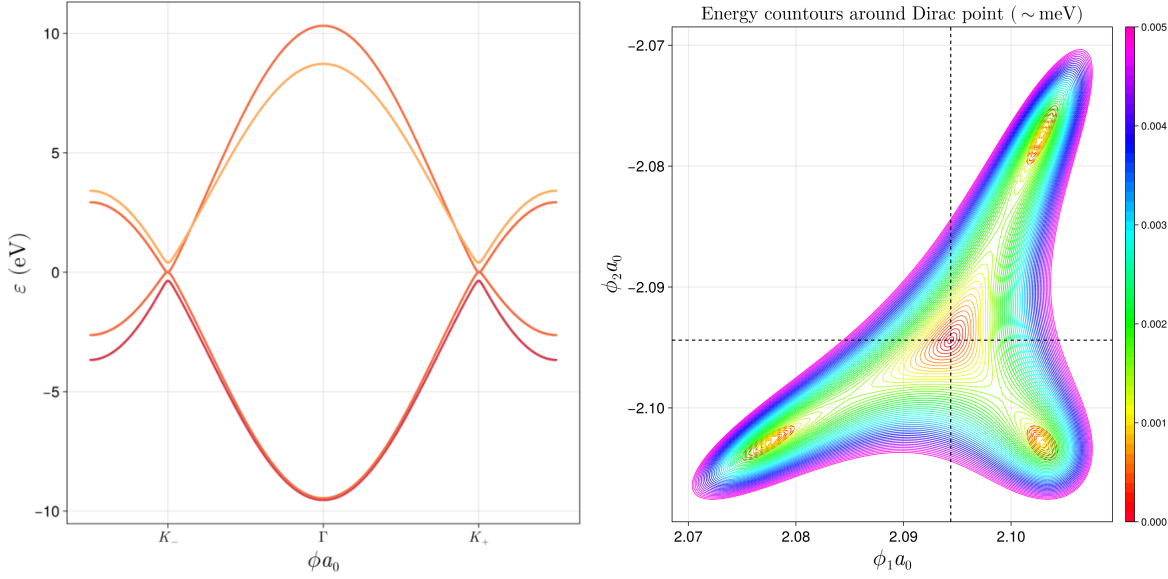


Figure 10. (a, b) Bandstructure along symmetry path $\Gamma \rightarrow K_+ \rightarrow M$ and (c) trigonal warping of BLG around the Dirac point K_+ .

Armchair and Zigzag configurations

3. Haldane model

4. Kekulé modulation

5. Twisted bilayer graphene